Clays and Clay Minerals, Vol. 53, No. 4, 409–421, 2005.

ORIGIN OF CLAY MINERALS IN SOILS ON PYROCLASTIC DEPOSITS IN THE ISLAND OF LIPARI (ITALY)

A. MIRABELLA[1,*], M. EGLI[2], S. RAIMONDI[3] AND D. GIACCAI[1]

[1]Istituto Sperimentale per lo Studio e la Difesa del Suolo – Piazza D'Azeglio 30, 50121 Firenze, Italy
[2]Department of Geography – Winterthurerstrasse 190, 8057 Zurich, Switzerland
[3]Dipartimento di Agronomia Ambientale e Territoriale, Università di Palermo – V.le delle Scienze, 90128 Palermo, Italy

Abstract—The island of Lipari (Italy) is characterized by calc-alkaline to potassic volcanism and a Mediterranean-type climate. The mineralogical and chemical features of two different soil profiles with ages of 92,000 and 10,000–40,000 y, respectively, have been investigated. There were no Andisols, but Vitric and Vertic Cambisols have developed at both sites. Although the morphology of the soils was similar, remarkable differences in the clay mineralogy between the two sites were observed. The site with the Vitric Cambisol was associated with the weathering sequence: glass → halloysite → kaolinite or interstratified kaolinite-2:1 clay minerals. Both sites had smectite in the clay fraction and, to a large extent, this smectite had a low charge and could be characterized as a dioctahedral montmorillonite. At the site with a Vertic Cambisol, smectite was the predominant mineral phase in the clay fraction. The smectites (predominantly montmorillonite) found in this soil were probably not of pedogenetic origin and are, therefore, inherited from the parent material. Their formation is due to hydrothermal alteration of glass particles during or immediately after the emplacement of the pyroclastic flow. The octahedral character of the smectites did not change from the C to the A horizon indicating that they are resistant to weathering processes. A high-charge expandable mineral was detected in small concentrations in the Vertic Cambisol and had a dioctahedral structure. In this case also, no signs of significant weathering or transformation could be detected in the soil profile. In contrast to many other investigations, no active smectite formation within the soil profiles could be measured. The subtropical and rather dry climate in Lipari might, therefore, favor the persistence of dioctahedral low-charge montmorillonites that are associated with a small amount of a high-charge expandable mineral in the soil.

Key Words—Halloysite, Kaolinite, Montmorillonite, Smectite, Volcanic Environment, Weathering.

INTRODUCTION

Pyroclastic deposits and volcanic ash give rise to weathering sequences where different soil types may coexist over relatively short distances. These parent materials might be associated with the weathering sequence of volcanic glass → allophane → halloysite → kaolinite (Parfitt *et al.*, 1983; Shoji *et al.*, 1993; Ndayiragije and Delvaux, 2004). Other clay minerals, such as smectites, can be found in volcanic soils and may be derived from hydrothermal processes (Bischoff, 1972; Pevear *et al.*, 1982; Inoue and Utada, 1983). The initial stage of glass alteration by aqueous solutions is characterized by a selective loss of alkalis. As alteration proceeds, clay minerals may form in the inner part of a glass or are due to a solid-state rearrangement in the hydrated layer or to precipitation from the solution (hydrothermal formation; Fiore *et al.*, 1999). Smectite, palygorskite, illite and interstratified illite-smectite are often found in volcanic deposits (Shoval, 2004; Altaner *et al.*, 2003; Prudêncio *et al.*, 2002). Smectite, illite and interstratified illite-smectite in soils developed on tephra may also derive from the alteration of primary minerals of tephra, from eolian contributions or are formed by pedogenetic weathering of X-ray amorphous materials (Fiore, 1993). Many authors surmise that smectites dominate among the clay minerals in soils developed on volcanic rocks (Craig and Loughman, 1964; Paquet, 1970; Vizcaíno *et al.*, 1979; Vidales *et al.*, 1985; Prudêncio *et al.*, 2002). According to these authors, smectites are a common weathering product. Primary minerals weather at different rates, resulting in smectites and halloysites. In some cases palygorskite occurs in small amounts and its presence may indicate climatic aridity (Velde, 1992; Paquet and Ruellan, 1993). Also, halloysite often dominates in climates with a distinct dry season (Ugolini and Dahlgren, 2003). Detailed analysis of clay minerals in volcanic environments is rarely performed (*e.g.* De La Fuente *et al.*, 2000). Only a few studies exist of the characteristics (*i.e.* charge and charge distribution) of smectites in such environments. Chemical and structural analyses of smectites from weathering profiles in central and southern Portugal revealed a montmorillonitic composition (Prudêncio *et al.*, 2002).

Many of the previously mentioned studies have been performed on soils with ages of >100,000 y up to several millions of years. We investigated volcanic soils in a

---

* E-mail address of corresponding author:
aldo.mirabella@issds.it
DOI: 10.1346/CCMN.2005.0530409

Mediterranean area (subtropical and periodically dry climate) with the aims to: (1) determine the main clay mineral formations and transformations; (2) discover whether smectite is actively formed during weathering in relatively young soils; and (3) specify in detail the structural properties of smectites. We investigated soil profiles on the volcanic island of Lipari (Italy), where the volcanic products are characterized by calc-alkaline to potassic volcanism (Crisci *et al.*, 1983) with ages <100,000 y.

INVESTIGATION AREA

The volcanic island of Lipari is the widest part of the Aeolian archipelago with an area of 38 km^2, and its morphology is related to the presence of many eruptive centers, characterized by different eruptive cycles. It is located north of Sicily and the highest point is Mount Chirica at 602 m a.s.l. Similarly to the other islands in the Aeolian arc, the volcanic products are derived from calc-alkaline to potassic volcanism, with a high gradient of K enrichment (Crisci *et al.*, 1983). The oldest rocks are dated at 223,000 y, while the most recent result from an eruption which took place ~1400 y ago. Volcanic activity at Lipari started 1000 m below sea level and it is still active, as demonstrated by the presence of low-temperature (80–90ºC) fumaroles and hot springs at the western side of the island. Intense hydrothermal activity on the western belt is documented by the kaolin mines exploited since ancient times.

The geology of Lipari is quite complex and is the result of a series of volcanic events that are related to two main evolution stages separated by an important stasis of volcanic activity between 92,000±10,000 and 45,000 y ago (Calanchi *et al.*, 1996). The western part, including the areas of Quattropani and Chiesa Vecchia, is ascribed to the pre-stasis period, demonstrating the effects of erosion processes, while the southern part (Falcone) is assigned to the post-erosion stage and, therefore, younger than 45,000 y.

The southern part of the island consists mainly of late-Pleistocene volcanic products of a pyroclastic-surge series, the Monte Guardia sequence, related to the extrusion of rhyolitic domes; fine-grained volcanic ash layers (brown tuffs) are found above and below this sequence (Crisci *et al.*, 1981). These deposits can be dated to 35,000–16,800 y.

The oldest outcrops are in the northwestern part of the island. They comprise lava and pyroclastites of basaltic-andesitic composition. With the formation of volcano S. Angelo (127,000–92,000 y ago) the eruptions became more explosive and the eruptive dynamics had a hydro-magmatic character. Climatic and pedoclimatic conditions as measured at the Santa Marina Station, located on the nearby island of Salina, for the period 1966–1994 are characterized by a mean annual temperature of 17.9ºC and mean annual precipitation of 637 mm. The climate, according to Thornthwaite and Mather (1957), is from sub-humid to sub-arid third mesothermic (C1B′3). The temperature regimen is thermic continental (15ºC $\leqslant T <$ 19ºC; Raimondi *et al.*, 1999) and the humidity regimen from intermediate xeric torric to xeric (Raimondi *et al.*, 1997).

MATERIALS AND METHODS

Two soils were selected, one in the southern (Osservatorio 1), and the other in the northern part (Quattropani 1) of the island (Figure 1). The soils were described and classified according to WRB (1998). Soil material was collected from excavated profile pits, air dried and sieved at 2 mm. Particle-size distribution was measured by the pipette method after dispersion with calgon® and sedimentation in deionized water. Bulk density was determined on undisturbed soil cores. The organic C content was estimated by the Walkley-Black method; soil pH by potentiometry in water and NaF, using a soil:solution ratio of 1:2.5. Total C content was measured using a C/H/N analyzer (Elementar Vario EL). The cation exchange capacity (CEC) and exchangeable bases were determined with a 1 N NH_4OAc extraction and the cations were analyzed by atomic absorption spectroscopy (AAS) (Soil Survey Staff, 2003). Phosphate retention was calculated as described by Blakemore *et al.* (1981). The Al, Fe and Si were extracted by NH_4 oxalate at pH 3 (Al_o, Fe_o, Si_o) (Schwertmann, 1964) and the Fe by dithionite-citrate-

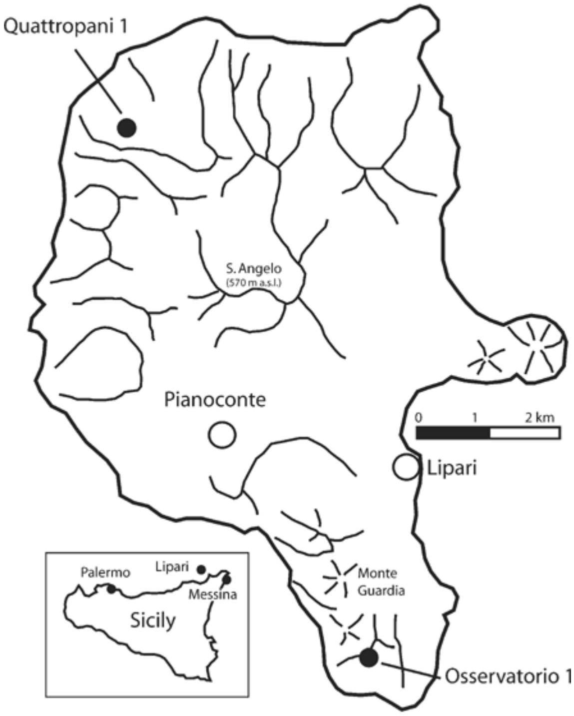

Figure 1. Locations of soil profiles on the island of Lipari.

bicarbonate (Fe_d) (Soil Conservation Service, 1972); Al, Fe and Si in solution were determined by AAS. Element pools in the soil (Ca, Mg, K, Na, Fe, Al, Mn, Si and Ti) were determined by a method of total dissolution. Oven-dried samples were dissolved using a mixture of HF, HCl, HNO_3 and H_3BO_3 as in Fitze *et al.* (2000). Concentrations of Ca, Mg, K, Na, Fe, Mn, Al, Si and Ti were determined by AAS, in part using a graphite furnace. Loss on ignition (LOI) was determined on 2.5 g of oven-dried (70°C for 2 h) soil material ignited at 900°C over a period of 2 h. Short-order Al-silicate components (ITM), *i.e.* the sum of imogolite and proto-imogolite allophane, were estimated according to the method suggested by Parfitt and Henmi (1982), *i.e.* as allophane + imogolite% = Si(oxalate)% × 7.1.

X-ray diffraction (XRD) was carried out on the clay fraction (<2 μm), obtained by dispersion with Calgon® and sedimentation in water. Specimens were then Mg saturated, washed free of chlorides and freeze dried. Clay-aggregate samples, oriented on glass slides from a water suspension, were analyzed using a 3 kW Rigaku D/MAX III C diffractometer, equipped with a horizontal goniometer, a curved-beam graphite monochromator and CuKα radiation. Slides were step-scanned from 2 to 15°2θ with steps of 0.02°2θ at 2 s intervals. The following treatments were performed: Mg saturation, ethylene glycol solvation and K saturation, followed by heating for 2 h at 335 and 550°C. To distinguish between kaolinite and interstratified kaolinite-2:1 clay minerals, the clay sample was intercalated with a 10% formamide in ethanol solution (Frost *et al.*, 1999). To distinguish between kaolinite and halloysite, intercalation complexes of both, created by immersing them in a 6.5 M K acetate solution for 18 days were used. The resulting complexes were washed with water until dispersion (Wada, 1961). After this process, halloysite (0.7 nm) will expand, resulting in greater *d* values, while kaolinite will collapse, if expanded by the intercalating procedure, to its original basal spacing close to 0.7 nm.

The 060 region was studied on random mounts prepared by filling the cavity of a glass holder and then step-scanned from 58 to 64°2θ with steps of 0.02°2θ at 10 s intervals. Diffraction patterns were smoothed by a Fourier transform function and fitted by the Origin™ PFM using the Pearson VII algorithm. Background values were calculated by means of a non-linear function (polynomial 2nd order function; Lanson, 1997).

Layer-charge estimation of smectites was performed using the long-chain alkylammonium ion C18 according to the method proposed by Olis *et al.* (1990).

For the monolayer to bilayer transition, equation 1 was used:

$$d_{001} = 8.21 + 34.22\xi \quad (1)$$

with ξ = mean layer charge and *d* values given in Å. For the bilayer to pseudotrimolecular layer transition, the equation is:

$$d_{001} = 8.71 + 29.65\xi \quad (2)$$

Values of layer charge calculated from *d* spacings >3.1 nm are beyond the limits of the C18 BTP regression model of Olis *et al.* (1990) and will, therefore, be indicated as >0.75 per half unit-cell.

To distinguish beidellitic from montmorillonitic smectites, the Mg-saturated clay samples were Li saturated, heated at 300°C overnight and then glycerol solvated (Greene-Kelly, 1953). To avoid reaction of the clay film with Na of the glass slide when it is heated at 300°C, the Li-saturated clay was heated in a platinum crucible. The sample was then resuspended in water and oriented on a glass slide.

RESULTS

Physical and chemical analyses

The soil profile Osservatorio 1 (in the southern part of the island; at an altitude of 210 m a.s.l.) is representative of the soils that develop from the pyroclastic deposits attributed to the volcanic activities between ~40,000 and 10,000 y B.P. (Table 1). The deposits, mainly pumiceous, in part constitute thin, moderately hard layers. The texture is sandy loam in the A horizon and sandy in the rest of the profile (Bw and C) (Table 2).

Bulk density ranges from 0.94 kg dm^{-3} in the A horizon to 0.99 kg dm^{-3} in the Bw horizon. The soil is slightly acid in the A horizon and the pH in water decreases with depth. The pH in NaF is always <9.5, indicating small amounts of X-ray amorphous Al-phases. Organic matter is common in the surface A horizon and its amount decreases with depth. The soil has a low cation exchange capacity (CEC) and base saturation is always >50%.

According to the WRB (1998), the investigated soil does not meet the Andic requirements, due to low phosphate retention (<70%), high bulk density (>0.90 kg dm^{-3}), and small amounts of X-ray amorphous compounds (the sum of $[Al_o+1/2Fe_o]$ <2%). Furthermore, the ITM content was small (Table 2). A typical rhyolitic composition was measured for this profile (Table 3) with large Si contents. The small variations within the soil profile showed that the deposited material was quite homogeneous.

The soil profile Quattropani 1 is representative of the soils that evolve on the pyroclastic deposits having an age of 92,000±10,000 y. The present pedological condition derives from the transformations of the pyroclastic deposits by a past thermalism. The individual pyroclastic particles are no longer visible in the soil horizons and are slightly weathered by pedogenetic processes. The texture in the soil is clayey-sandy in the A horizon, clayey in the Bw horizon and sandy-loamy in the C horizon (Table 2). The soil is slightly acid in the surface A horizon and neutral in the other two horizons. The pH

Table 1. Characteristics of the two study sites (Lipari island, Italy).

Location	Elevation (m a.s.l.)	Aspect (°N)	Slope (%)	Parent material	Age (years)	Land use	Vegetation	WRB* (1998)
Osservatorio 1	210	180	50	Pyroclastic, rhyolitic deposits	10,000–40,000	Pasture and low bush, cistus	*Hiparrenia irta, Inula viscosa, Lupinus linifolius*	Vitric Cambisol
Quattropani 1	300	300	<5	Pyroclastic, andesitic-basaltic deposits	92,000	Abandoned cultivated land	*Hedysarum coronarium, Artemisia arborescens, Dactilis glomerata, Avena fatua, Feniculum piperitum, Inula viscosa*	Vertic Cambisol

*World reference base, for soil resources

Table 2. Physical and chemical characteristics of the investigated soils.

Horizon	Clay	Silt	Sand	pH H_2O	pH NaF	Bulk density	C*	P ret.	Fe_d	Fe_o	Al_o	Si_o	ITM†	CEC	Na	K	Ca	Mg	Base sat.
(cm)	—	$(g\ kg^{-1})$	—			$(kg\ dm^{-3})$	$(g\ kg^{-1})$	(%)	—	—	$(g\ kg^{-1})$	—	—	—	—	$(cmol_c\ kg^{-1})$	—	—	(%)
Osservatorio 1																			
A (0–15)	42	94	864	6.4	7.9	0.94	7	46.3	4.1	1.9	0.7	1.5	10.7	13.1	1.9	0.4	4.0	1.8	62
Bw (15–50)	38	103	858	5.5	7.6	0.99	5	43.5	3.4	0.9	0.4	1.5	10.7	11.0	1.2	0.3	3.1	1.3	54
C (50–95)	36	175	789	5.6	7.6	n.d.	1	40.1	2.3	1.5	0.5	0.7	5.0	8.1	1.0	0.3	2.6	0.8	59
Quattropani 1																			
A (0–15)	401	284	315	6.5	7.8	1.30	18	38.8	12.0	1.3	0.6	1.5	10.7	29.4	1.3	1.2	12.5	5.6	70
Bw (15–50)	395	305	300	6.8	8.2	1.41	6	48.9	11.1	1.5	0.5	0.8	5.7	28.7	2.2	1.1	14.5	1.9	69
C (50–75)	179	376	446	7.2	8.3	n.d.	n.d.	43.2	6.3	1.0	0.7	0.9	6.4	29.0	1.4	1.2	16.0	1.8	70

* Walkley-Black method
† ITM = imogolite-type material
n.d. = not detected

Table 3. Total elemental contents (g kg^{-1}) of the investigated soils (fine earth).

Horizon (cm)	SiO_2	Al_2O_3	Fe_2O_3	MnO	Na_2O	K_2O	CaO	MgO	TiO_2	LOI	Org. matter*	IVC†
Osservatorio 1												
A (0–15)	659.9	147.1	36.5	0.87	27.7	38.7	12.6	9.6	3.59	40.1	10.8	29
Bw (15–50)	702.0	133.9	24.0	0.58	30.8	43.3	8.0	4.5	1.81	43.2	8.7	35
C (50–95)	691.9	132.6	17.3	0.45	31.4	46.7	5.2	1.3	1.27	29.6	1.2	28
Quattropani 1												
A (0–15)	507.5	162.5	75.9	0.76	11.5	10.4	26.6	24.9	10.15	150.8	26.8	124
Bw (15–50)	505.7	168.2	76.7	0.64	10.8	9.3	24.3	25.7	10.93	150.1	11.7	138
C (50–75)	554.0	151.3	53.5	0.13	4.9	4.8	10.3	21.3	12.18	185.5	1.2	184

* organic matter = total organic C × 1.72; total organic C was determined by a CHN analyzer

† inorganic volatile compounds, estimated by LOI (loss on ignition) – organic matter

value in NaF is always <9.5. Bulk density is high. The amount of organic C is greater in the surface horizon and decreases noticeably with depth. The CEC is moderate and the base saturation is near 70%. Phosphate retention is low. The sum of X-ray amorphous Al + 1/2 of X-ray amorphous Fe (Al_o+1/2Fe_o) is always <2%. Given these characteristics, the soil does not meet the Andic requirements. The ferrihydrite content (estimated by Fe_o) is small (Table 2). The amount of allophane, as determined by the oxalate-extractable Si (Si_o), is small. The amount of Al_o is also very small. The relatively high values of Fe_d-Fe_o indicate that Fe is mostly present in a crystalline form. The chemical composition within the soil profile does not vary greatly (Table 3). This shows that the pyroclastic deposits had a more or less similar chemical and andesitic composition. In contrast to the Osservatorio 1 profile, this soil had a comparatively small Si content but a greater inorganic volatile compounds content. Also, the Fe and Al contents are slightly greater. Furthermore, the distribution of base cations is different with smaller Na and K contents but greater Ca and Mg contents at this site. In the soil profile the amount of inorganic volatile compounds decreases steadily from the parent material to the surface.

Clay mineral analyses

The XRD pattern of the EG-solvated sample from the surface A horizon of the Osservatorio 1 soil profile is characterized by an intense broad peak at ~0.74 nm. K saturation and heating at 335ºC caused narrowing of the peak. Because of its broad shape, position and disappearance after the heat treatment at 550ºC, this peak could be assigned to dehydrated halloysite or disordered kaolinite, or both. The other peaks present were at 1.01 and 1.67 nm, belonging to mica and smectite, respectively (Figure 2). The peak of the smectitic component appeared very broad and not very intense. Therefore, this component is present in small amounts and is characterized by particles of small dimension in the direction perpendicular to the basal planes.

The clay mineralogy of the two lower horizons (Bw and C) is very similar to that of the surface horizon. In the lowest C horizon the peak around 0.74 nm is now broader, while the peak at 0.65 nm, belonging to plagioclase, is more evident (Figure 2).

The clay mineral composition of the Quattropani 1 soil was found to be different from that of the Osservatorio 1 soil. The XRD pattern of the EG-solvated sample of the surface A horizon was characterized by a distinct and intense peak at 1.73 nm which collapsed to 1.47 nm following Mg saturation and to 1.26 nm after the K treatment. The peak collapsed to 1.0 nm following heat treatment at 335ºC (Figure 2). Because of these features, this component was identified as a low-charge expandable clay mineral. The narrow peak indicates that a large dimension in the direction perpendicular to the basal planes is characteristic of this smectite. It is possible that the presence of a small amount of a high-charge expandable mineral is indicated by a very small peak at 1.0 nm in the XRD pattern of the K-saturated sample. In the XRD pattern of the EG-solvated sample, a peak at 0.87 nm, which disappears in the Mg-saturated sample, represents the d_{002} reflection of the same expandable mineral. A small amount of kaolinite was also present in this horizon, as denoted by the peak at 0.72 nm, which disappears after the heat treatment at 550ºC. The two underlying horizons (Bw and C) showed a clay mineral composition similar to that of the surface horizon (Figure 2).

Formamide intercalation, performed on the clay sample from the surface A horizon of the profile Osservatorio 1, caused the partial expansion to 0.96 nm of the peak around 0.74 nm. Therefore, the residual peak at 0.75 nm could be assigned to an interstratified kaolinite- or halloysite-2:1 clay mineral, or to a kaolinite mineral resistant to the intercalation with formamide, while the expanded peak could belong to halloysite or kaolinite or both (Figure 3). The K acetate intercalation did not produce any expansion of the peak at 0.70 nm and therefore this peak could be assigned to kaolinite (Figure 3). The clay sample from the Bw horizon underneath had a similar behavior to that of the surface A horizon (Figure 3). The peak at ~0.75 nm of the clay sample from the lowest C horizon

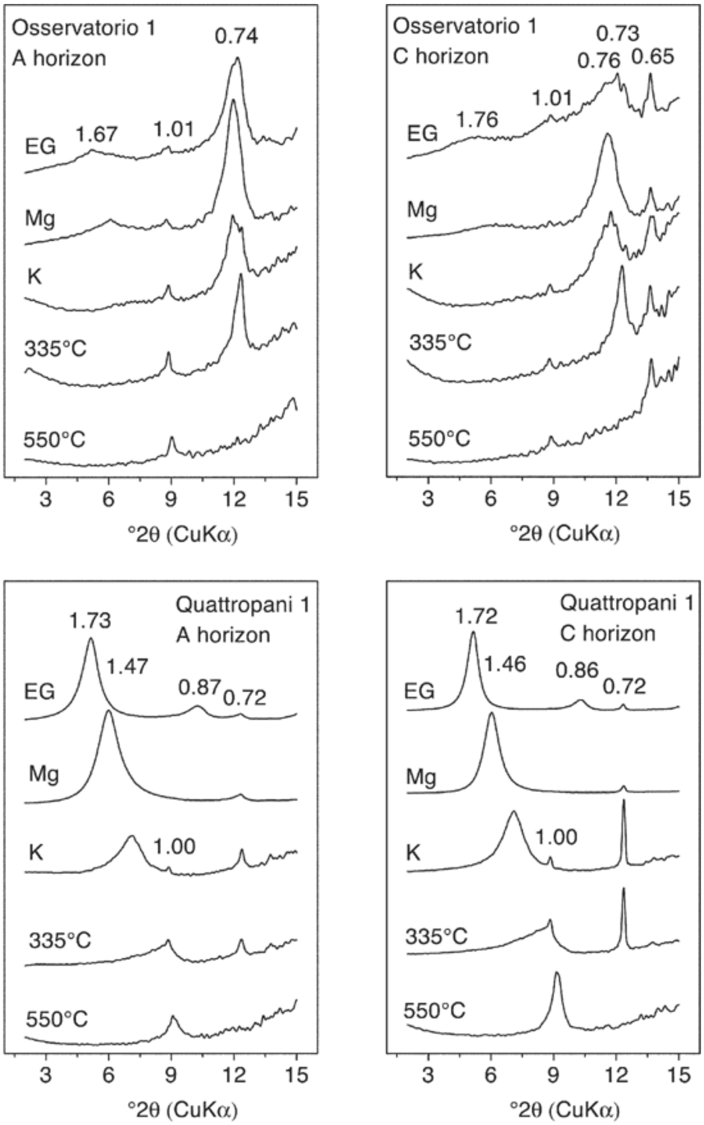

Figure 2. XRD patterns of the <2 μm clay samples from the A and C horizons of the two soil profiles Osservatorio 1 and Quattropani 1. The XRD patterns are smoothed and corrected for Lorentz and polarization factors. The *d* spacings are given in nm. EG = ethylene glycol solvation, Mg = Mg saturation, K = K saturation and corresponding heating treatments.

expanded completely after the formamide intercalation, indicating that there was no interstratification between kaolinite or halloysite with 2:1 clay minerals. The K acetate intercalation produced an almost complete expansion of this peak that was, therefore, assigned to halloysite, while the residual peak at 0.71 nm belongs to kaolinite.

The formamide intercalation caused the expansion of the peak at 0.72 nm in all the horizons of the Quattropani 1 soil profile (Figure 4), while the K acetate failed to expand these components (Figure 4); therefore, kaolinite could be identified throughout the soil profile.

The XRD patterns of the 060 region showed that almost all clay minerals in the Osservatorio 1 soil are dioctahedral. In fact, no intense peaks could be detected in the region of trioctahedral species in the *d* spacing range 0.1538–0.1550 nm (Moore and Reynolds, 1997). In the sample of the A horizon, an intense peak was present, centered at 0.1491 nm, that can be attributed to the 1:1 clay mineral (Figure 5). The same peak was present in the lower Bw and C horizons. All the XRD patterns showed a shoulder towards higher angles that was resolved in a weaker peak in the range 0.1474–0.1478 nm, probably belonging to a different phase of the 1:1 clay mineral, while the small peak around 0.1510–0.1513 nm could belong to the smectitic component (Figure 5).

The Quattropani 1 soil showed no evidence of the presence of trioctahedral species. In all the clay samples of this soil, the 060 XRD peak maxima were located at lower angles, when compared to the clay sample from the Osservatorio 1 soil (Figure 5). The value of the most intense peak was centered around 0.1500 nm and belongs to the low-charge expandable mineral. The less intense peak in the range 0.1490−0.1486 nm could be assigned to kaolinite, present in this soil in small amounts (Figure 5).

The Greene-Kelly test applied to Osservatorio 1 soil samples did not give any identifiable variation in the XRD patterns (not shown) of the clay samples which were Li saturated, heated to 300ºC and solvated with glycerol, indicating that the small amount of smectite had a montmorillonitic composition.

The Greene-Kelly test was also applied to the samples of Quattropani 1 soil. Li saturation and the heat treatment at 300ºC caused a shift of the peak which was centered at 1.73 nm in the XRD pattern of the EG-solvated samples, to 1.5 and 0.98 nm, respectively (Figure 6). The solvation with glycerol, which followed, did not cause any expansion of the peak at 0.98 nm (Figure 6). This indicates that the smectite had a predominantly montmorillonitic nature, because Li has entered into the octahedral sheet and has transformed the smectite into a pyrophyllite-like phase (Moore and Reynolds, 1997). The peak at 0.98 nm was quite broad, with a shoulder towards lower angles; therefore, some of the smectitic components showed some resistance to collapse to 0.98 nm after Li saturation and the heating treatment (Figure 6). The Greene-Kelly test applied to the lower Bw and C soil horizons of this profile gave similar results (Figure 6).

Layer-charge diffraction patterns, obtained with the long-chain alkylammonium ion C18 intercalation, showed for the Osservatorio 1 soil profile peaks with low intensities in the area of interest for the calculation of the charge. Two peaks could, however, be separated in the surface A horizon centered at 2.16 and 1.86 nm, respectively (Figure 7). The values of these *d* spacings correspond to layer charges (ξ) of 0.39 and 0.30. Therefore, the 2:1 clay minerals comprise mainly two low-charge components. The Bw horizon showed a mixture of mineral phases, with charges ranging from >0.75 to 0.32. The deeper C horizon showed the same range of charges as the Bw horizon (Figure 7).

The fitting procedure, carried out on the clay sample from the surface A horizon of Quattropani 1 soil profile

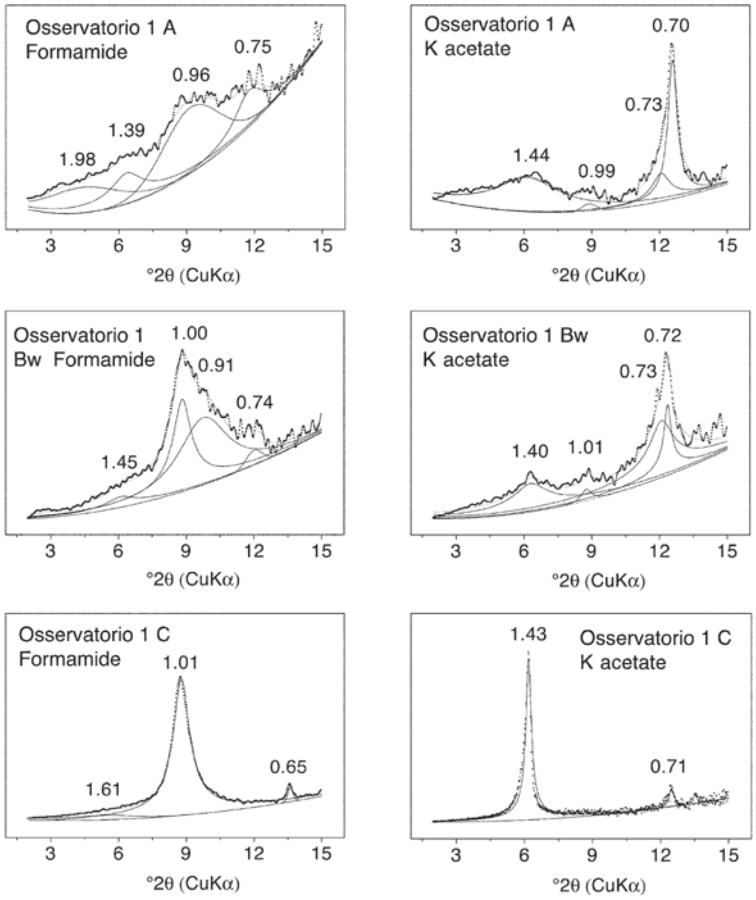

Figure 3. XRD patterns of the <2 μm clay samples from the A, Bw and C horizons of the soil profile Osservatorio 1. The clay samples are intercalated with formamide and K acetate, respectively. The XRD curves are corrected for Lorentz and polarization factors. The *d* values are given in nm.

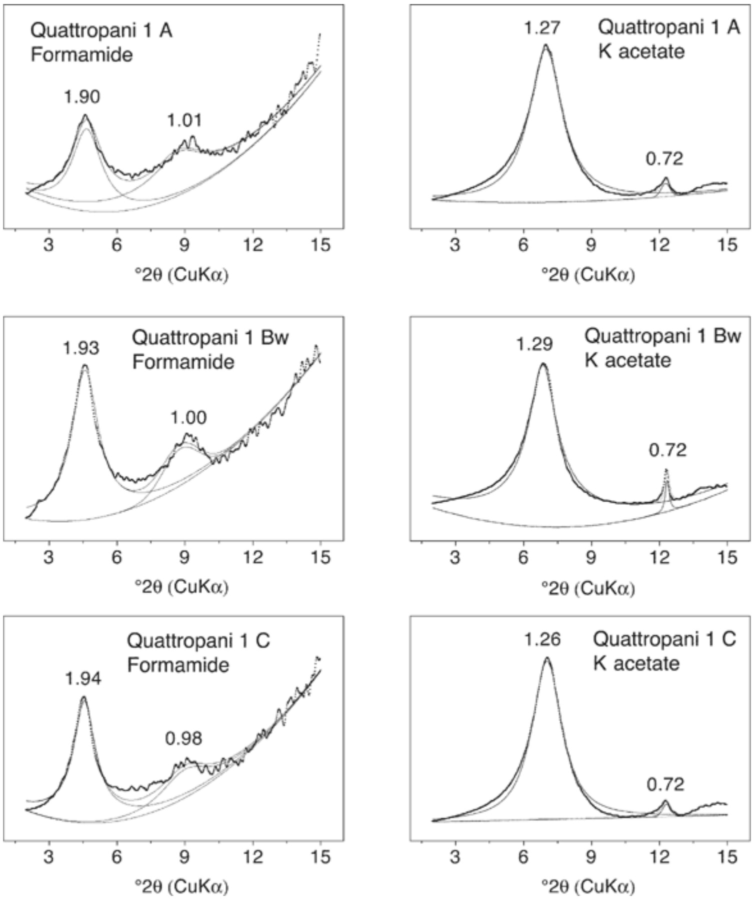

Figure 4. XRD patterns of the <2 μm clay samples from the A, Bw and C horizons of the soil profile Quattropani 1. The clay samples are intercalated with formamide and K acetate, respectively. The XRD patterns are corrected for Lorentz and polarization factors. The *d* values are given in nm.

intercalated with the C18 alkylammonium, allowed the identification of a peak with a *d* spacing of 2.00 nm, corresponding to a layer charge (ξ) of 0.34 (Figure 7). The XRD pattern of the clay sample from the Bw horizon, intercalated with C18 alkylammonium, gave a peak centered at 1.97 nm. In this case also, the calculated charge by the use of the BTP model was 0.34. The C horizon gave a similar result with a calculated layer charge per half unit-cell of 0.36 (Figure 7).

DISCUSSION

Weathering of individual soils differs due to varying soil properties and surrounding environmental conditions. This is expressed by the well known and fundamental theory of Jenny (1980), according to which the soil characteristics are determined by the factors: parent material, climate, topography, the age of the soil and the organisms. The physical, chemical and mineralogical results have shown that the two soils developing in the island of Lipari have different properties. These differences might be attributed both to the different age of the soils (Osservatorio 1 at 40,000–10,000 y and Quattropani 1 at 92,000 y) or to the intrinsic characteristics of pyroclastic flows as the climate and vegetation are similar for the two soils.

The CEC was greater in the Quattropani soil, where the greater organic carbon content may contribute. Both soils had a large base saturation and contain small amounts of X-ray amorphous phases, as indicated by the small percentage of oxalate-extractable Al and Si. The allophanic components content and the X-ray amorphous Fe oxides content were small in both soils.

The greater clay content at Quattropani 1 could be due to: (1) the chemical, mineralogical and physical properties of the parent material; (2) the post-depositional weathering environment, and (3) the stage of soil formation (Dahlgren *et al.*, 1993). All these conditions are possible.

The two soils showed different clay mineralogies; 1:1 clay minerals were mainly present in the soil profile Osservatorio 1, together with a small amount of a smectitic component whereas a well crystallized low-charge smectite dominated the XRD patterns of the clay fraction of the soil profile Quattropani 1.

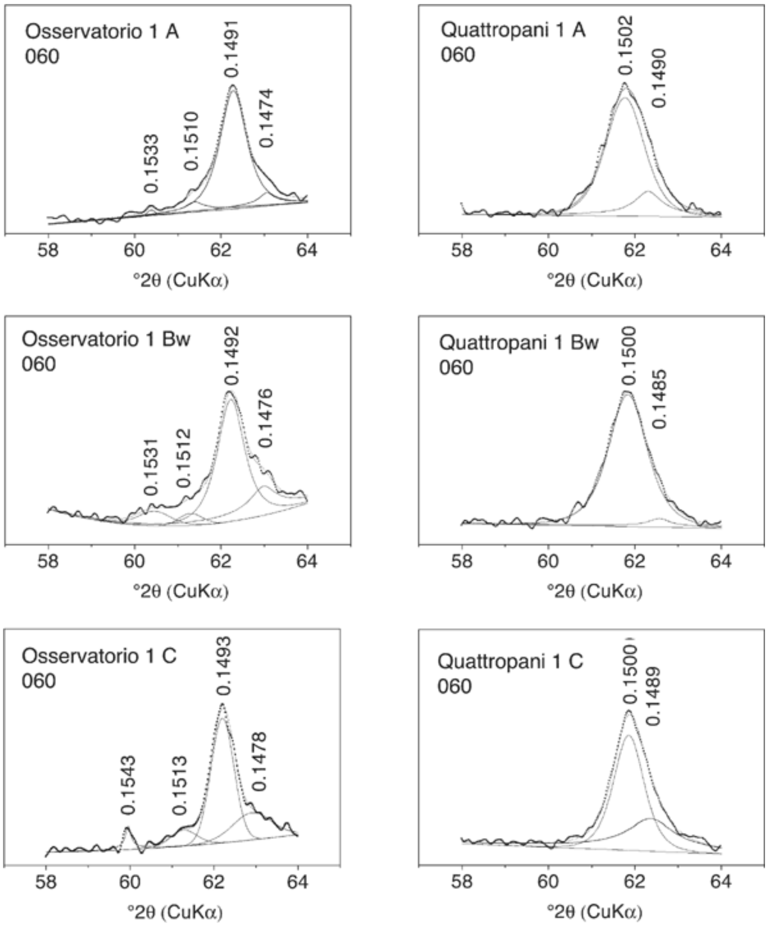

Figure 5. Deconvolution of XRD peaks in the d_{060} region of the <2 μm clay samples from the A, Bw and C horizons of the two soil profiles Osservatorio 1 and Quattropani 1. The d values are given in nm.

The following main transformation reactions in the soils can be suggested:

Osservatorio 1

Transformation with time of halloysite → kaolinite together with an interstratification of kaolinite with 2:1 clay minerals. Halloysite found in this profile has probably been formed by syneruptive glass alteration initiated by fluids during or immediately after the emplacement of pyroclastic flow materials (Fiore, 1993). Hydrothermal activity is not essential for the formation of kaolinite and halloysite (Dixon, 1989), but has been reported as an environmental factor where these clays have formed in Japan, Korea, Mexico (Minato *et al.*, 1982) and in the Hawaiian Islands. Hay (1960) and McIntosh (1979) suggested that halloysite can form in <4000 y and <2500 y, respectively. Under the present environmental conditions in Lipari, halloysite does not seem to be stable and therefore transforms into kaolinite; a process similar to that observed by Singer *et al.* (2004). This is also in agreement with Parfitt *et al.* (1983) and Quantin (1990) who showed that hydrated halloysite represents a less advanced weathering stage than kaolinite. Some of the kaolinite might have been formed directly from the weathering and dissolution of plagioclase which cannot, however, be fully proved with our data.

Quattropani 1

Almost no variation in the clay mineral assemblage is observable from the C to the A horizon. The clay minerals consist primarily of a low-charge smectite. A smaller amount of kaolinite and of a high-charge expandable mineral are also present. The clay minerals are therefore relatively stable in the present environmental conditions.

Both sites are characterized by a prevalence of dioctahedral minerals in the clay fraction. Dioctahedral minerals generally have greater resistance to weathering than trioctahedral phases (cf. Egli *et al.*, 2001). In both soils, only minor modifications were discernible from the C to the A horizon in the d_{060} region.

As regards the genesis of the 2:1 clay minerals, their presence in volcanic soils is debated. Three hypotheses

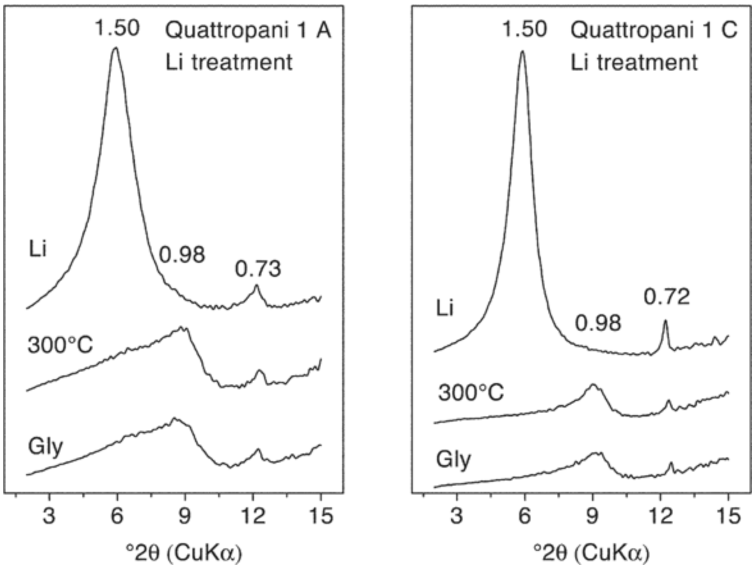

Figure 6. XRD patterns of the <2 µm clay samples from the A and C horizons of the soil profile Quattropani 1 treated according to the Greene-Kelly test. The XRD patterns are corrected for Lorentz and polarization factors. The *d* values are given in nm. Li = Li saturation and corresponding heating treatment; Gly = glycerol solvation of the Li-saturated and heated sample.

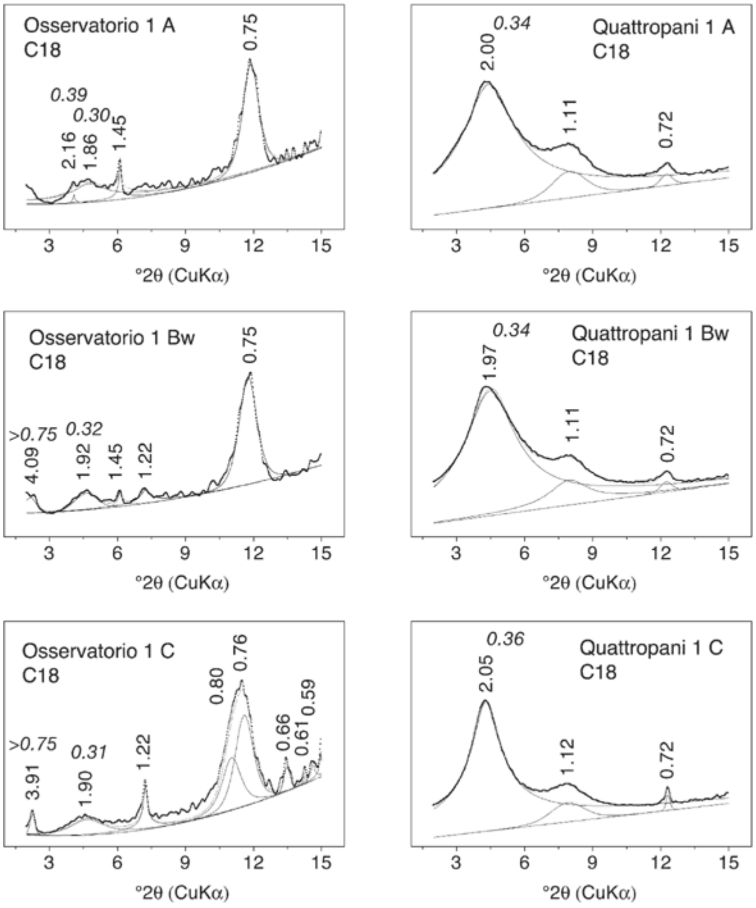

Figure 7. XRD patterns of the <2 µm clay samples from the A, Bw and C horizons of both profiles treated with C18 (18-alkylammonium ion). The XRD curves are corrected for Lorentz and polarization factors. The *d* values are given in nm. The italicized numbers indicate the calculated layer charge per half unit-cell

are suggested: (1) clay minerals can originate or be inherited from the primary minerals of tephra; (2) they could be part of an eolian contribution or weathered from them; or (3) they are pedogenetic products that crystallized from X-ray amorphous phases (Fiore, 1993). That author suggested that, in the volcanic area of Mt. Vulture in southern Italy, smectite and illite were formed during the emplacement of the pyroclastic flow under hydrothermal conditions. Smectite which originated from the weathering of volcanic ash samples (collected in Japan) under hydrothermal alteration within volcanic vents was reported by Mizota and Faure (1998) and experimental alteration of volcanic tuff at ~82ºC confirms this assumption (Cuadros *et al.*, 1999). Furthermore, *in situ* formation of smectite in channels of pumiceous particles might be possible (Chichester *et al.*, 1969; Cortes and Franzmeier, 1972). Additionally, Glassmann (1982) showed that smectite authigenesis can take place in voids left by augite and plagioclase dissolution in andesite cobbles. Freshly fallen volcanic ash from Mount St. Helens contained hydrothermally derived Fe-rich saponite (Pevear *et al.*, 1982; Borchardt, 1989). Extensive hydrothermal alteration may lead to clay-rich products, particularly kaolinite or smectite (Frank, 1983) at or near the ground surface.

It is likely that the smectite in the Quattropani soil profile was formed by the hydrothermal mechanism suggested and therefore is not of pedogenetic origin but is inherited from the parent material. Furthermore, the structure characteristics of smectite remained homogeneous throughout the profile, *e.g.* the low layer charge and the location of the charge. This indicates that the smectitic component is very stable in this pedogenic environment. Although beidellites are more common in soil environments, whereas montmorillonites are more typical of geological material (Wilson, 1987), montmorillonitic structures are able to persist in the surrounding acidic conditions of the investigated soils.

Investigations by Prudêncio *et al.* (2002) in Portugal showed that the degree of aridity may affect the stability of smectites which seem to evolve either to palygorskite or to analcime. Theoretically, a similar evolution should also be expected in Lipari (similar climate). However, the parent material and evolving soils studied there were much older than in this study. Shoval (2004) observed that palygorskite can occasionally be found associated with sepiolite. According to that author, smectite also transforms with time into interstratified illite-smectite (rich in smectite). Well developed smectitic soils are mostly restricted to dry tropical climates with an annual precipitation of 500–800 mm and a distinct dry season, along with poorly drained landscapes (Boulet *et al.*, 1997). The subtropical and rather dry climate in Lipari might, therefore, favor the persistence of smectites in the soil.

The smectites found in both soils are inherited from the parent material. The chemical and structural analyses of smectites revealed a mostly dioctahedral, low-charge montmorillonitic composition. The octahedral character of these minerals did not change from the C to the A horizon; therefore, they are resistant to weathering processes in the Lipari region.

CONCLUSIONS

The younger soil (with an age between 10,000 and 40,000 y) showed no sign of active smectite formation. In Mediterranean climates (subtropical with periods of drought), obviously more time is required for smectites to form pedogenetically from rhyolitic parent materials. First reactions include the transformation of halloysite into kaolinite. The other site contained a large amount of smectite in the parent material. The clay mineral assemblage was, however, relatively unaffected after 92,000 y of soil evolution. Dioctahedral, low-charge smectites of montmorillonitic structure seem to be relatively stable and resistant to weathering. It seems that they have neither been produced actively during soil evolution nor destroyed or transformed.

ACKNOWLEDGMENTS

The authors are grateful to Leonardo Leoni, Saverio Fiore, an unknown reviewer and Associate Editor Helge Stanjek, whose corrections and suggestions notably improved the manuscript.

REFERENCES

Altaner, S.P., Ylagan, R.F., Savin, S.M., Aronson, J.L., Belkin, H.E. and Pozzuoli, A. (2003) Geothermometry, geochronology, and mass transfer associated with hydrothermal alteration of a rhyolitic hyaloclastite from Ponza Island, Italy. *Geochimica et Cosmochimica Acta*, **67**, 275–288.

Bischoff, J.L. (1972) A ferroan nontronite from the Red Sea geothermal system. *Clays and Clay Minerals*, **20**, 217–223.

Blakemore, L.C., Searle, P.L. and Daly, B.K., (1981) *Soil bureau laboratory methods. A: Methods for chemical analysis of soils.* New Zealand Soil Bureau Scientific Report 10A, CSIRO, Lower Hutt, New Zealand.

Borchardt, G. (1989) Smectites. Pp. 675–727 in: *Minerals in Soil Environments* (J.B. Dixon and S.B. Weed, editors). Soil Science Society of America Book Series, Madison, Wisconsin.

Boulet, R., Lucas, Y., Fritsch, E. and Paquet, H. (1997) Geochemical processes in tropical landscapes: role of the soil covers. Pp 67–96 in: *Soils and Sediments: Mineralogy and Geochemistry* (H. Paquet and N. Clauer, editors). Springer Verlag, Berlin.

Calanchi, N., Luigi Rossi, P., Sanmarchi, F. and Tranne A. (1996) *Guida escursionistica vulcanologia delle isole Eolie.* Centro studi e ricerche di storia e problemi eoliani. Union Printing S.p.A., Viterbo p. 213.

Chichester, F.W., Youngberg, C.T. and Harward, M.E. (1969) Clay mineralogy of soils formed on Mazama pumice. *Soil Science Society of America Proceedings*, **33**, 115–125.

Cortes, A. and Franzmeier, D.P. (1972) Climosequence of ash-derived soils in the central cordillera of Colombia. *Soil Science Society of America Proceedings*, **26**, 653–659.

Craig, D.C. and Loughman, F.C. (1964) Chemical and mineralogical transformations accompanying the weathering of basic volcanic rocks from New South Wales. *Australian Journal of Soil Research*, **2**, 218–234.

Crisci, G.M., De Rosa, R., Lanzafame, G., Mazzuoli, R., Sheridan, M.F. and Zuffa, G.G. (1981) Monte Guardia sequence: a late-Pleistocene eruptive cycle on Lipari (Italy). *Bulletin of Volcanology*, **44**, 241–255.

Crisci, G.M., Delibrias, G., De Rosa, R., Mazzuoli, R. and Sheridan, M.F. (1983) Age and petrology of the late-Pleistocene Brown Tuffs on Lipari, Italy. *Bulletin of Volcanology*, **46**, 381–391.

Cuadros, J., Caballero, E., Huertas, F.J., De Cisneros, C.J., Huertas, F. and Linares, J. (1999) Experimental alteration of volcanic tuff: smectite formation and effect on ^{18}O isotope composition. *Clays and Clay Minerals*, **47**, 769–776.

Dahlgren, R., Shoji, S. and Nanzyo, M. (1993) Mineralogical characteristics of volcanic ash soils. Pp. 101–143 in: *Volcanic Ash Soils. Genesis, Properties and Utilization* (S. Shoji, M. Nanzyo and R. Dahlgren, editors). Developments in Soil Science **21**, Elsevier Science Publishers, Amsterdam, The Netherlands.

De La Fuente, S., Cuadros, J., Fiore, S. and Linares, J. (2000) Electron microscopy study of volcanic tuff alteration to illite-smectite under hydrothermal conditions. *Clays and Clay Minerals*, **48**, 339–350.

Dixon, J.B. (1989) Kaolin and Serpentine Group Minerals. Pp. 467–525 in: *Minerals in Soil Environments* (J.B. Dixon and S.B. Weed, editors). Soil Science Society of America Book Series, Madison, Wisconsin.

Egli, M., Mirabella, A. and Fitze, P. (2001) Clay mineral formation in soils of two different chronosequences in the Swiss Alps. *Geoderma*, **104**, 145–175.

Fiore, S. (1993) The occurrences of smectite and illite in a pyroclastic deposit prior to weathering: implications on the genesis of 2:1 clay minerals in volcanic soils. *Applied Clay Science*, **8**, 249–259.

Fiore, S., Genovese, G. and Miano, T.M. (1996) Organic matter migration and halloysite formation in pyroclastic deposits from Mt. Vulture (southern Italy). Pp. 108–109 in: *Advances in Clay Minerals* (M. Ortega-Huertas, A. López-Galindo and I. Palomo-Delgado, editors). University of Granada, Spain.

Fiore, S., Huertas, F.J., Tazaki, K., Huertas, F. and Linares, J. (1999) A low temperature experimental alteration of a rhyolitic obsidian. *European Journal of Mineralogy*, **11**, 1–5.

Fitze, P., Kägi, B. and Egli, M. (2000) *Laboranleitung zur Untersuchung von Boden und Wasser*. Geographisches Institut der Universität Zürich, Zürich, Switzerland.

Frank, D. (1983) Origin, distribution, and rapid removal of hydrothermally formed clay at Mount Baker, Washington. *Geological Survey Professional Paper* **1022-E**, pp. 1–31.

Frost, R.L., Lack, D.A., Paroz, G.N. and Tran, T.H.T. (1999) New techniques for studying the intercalation of kaolinites from Georgia with formamide. *Clays and Clay Minerals*, **47**, 297–303.

Glassmann, J.R. (1982) Alteration of andesite in wet, unstable soils of Oregon's western Cascades. *Clays and Clay Minerals*, **30**, 253–263.

Greene-Kelly, R. (1953) The identification of montmorillonoids in clays. *Journal of Soil Science*, **4**, 233–237.

Hay, R.L. (1960) Rate of formation and mineral alteration in a 4000-year-old ash soil of St. Vincent. *American Journal of Science*, **258**, 354–368.

Inoue, A. and Utada, M. (1983) Further investigations of a conversion series of dioctahedral mica/smectites in the Shinzan hydrothermal alteration area, Northeast Japan. *Clays and Clay Minerals*, **31**, 401–412.

Jenny, H. (1980) *The Soil Resource*. Springer, New York.

Lanson, B. (1997) Decomposition of experimental X-ray diffraction patterns (profile fitting): a convenient way to study clay minerals. *Clays and Clay Minerals*, **45**, 132–146.

McIntosh, P.D. (1979) Halloysite in a New Zealand tephra and paleosol less than 2500 years old. *New Zealand Journal of Science*, **22**, 49–54.

Minato, H., Kusakabe, H. and Inoue, A. (1982) Alteration reactions of halloysite under hydrothermal conditions with acidic solutions. Pp. 565–572 in: *Proceedings of the International Clay Conference 1981* (H. van Olphen and F. Veniale, editors). Elsevier, New York.

Mizota, C. and Faure, K. (1998) Hydrothermal origin of smectite in volcanic ash. *Clays and Clay Minerals*, **46**, 178–182.

Moore, D.M. and Reynolds, R.C. (1997) *X-ray diffraction and the Identification and Analysis of Clay Minerals*, 2nd edition. Oxford University Press, New York.

Ndayiragije, S. and Delvaux, B. (2004) Selective sorption of potassium in a weathering sequence of volcanic ash soils from Guadeloupe, French West Indies. *Catena*, **56**, 185–198.

Olis, A.C., Malla, P.B. and Douglas, L.A. (1990) The rapid estimation of the layer charges of 2:1 expanding clays from a single alkylammonium ion expansion. *Clay Minerals*, **25**, 39–50.

Paquet, H. (1970) Evolution géochimique des minéreaux argileux das les altérations et des sols des climats méditerranéens tropicaux à saisons contrastées. Thèse, Université de Strasbourg, Memoires de la Service Carte Geologique Alsace Lorraine, Strasbourg, France.

Paquet, H. and Ruellan, A. (1993) Epigenie des encroûtement calcaires (calcrètes). Pp. 19–39 in: Coll. '*Sédimentologie et Géochimie de la Surface*' à la Mémoire de Georges Millot (N. Clauer and H. Paquet, editors). Elsevier, Amsterdam.

Parfitt, R.L. and Henmi, T. (1982) Comparison of an oxalate-extraction method and an infrared spectroscopic method for determining allophane in soil clays. *Soil Science and Plant Nutrition*, **28**, 183–190.

Parfitt, R.L., Russel, M. and Orbell, G.E. (1983) Weathering sequence of soils from volcanic ash involving allophane and halloysite, New Zealand. *Geoderma*, **29**, 41–57.

Pevear, D.R., Dethier, D.P. and Frank, D. (1982) Clay minerals in the 1980 deposits from Mount St. Helens. *Clays and Clay Minerals*, **30**, 241–252.

Prudêncio, M.I., Sequeira Braga, M.A., Paquet, H., Waerenborgh, J.C., Pereira, L.C.J. and Gouveia, M.A. (2002) Clay mineral assemblages in weathered basalt profiles from central and southern Portugal: climatic significance. *Catena*, **49**, 77–89.

Quantin, P. (1990) Specificity of the halloysite-rich tropical or subtropical soils. *Transactions, 14th International Congress of Soil Science, Kyoto, 1990*, VII, pp. 16–21.

Raimondi, S., Lupo, M. and Tusa, D. (1999) Il clima ed il pedoclima dei suoli vulcanici dell'Etna. *Sicilia Foreste VI*, **23/24**, 2–7.

Raimondi, S., Poma, I. and Frenda, A.S. (1997) Il pedoclima come fattore di sensibilità ambientale: esempio di metodologia applicata all'agro di Sparacia – Cammarata (AG). *Rivista di Agronomia*, **XXXI**, 726–733.

Schwertmann, U. (1964) Differenzierung der Eisenoxide des Bodens durch Extraction mit Ammoniumoxalat Lösung. *Zeitschrift Pflanzenernährung Düng Bodenkunde*, **105**, 195–202.

Shoji, S., Nanzyo, M. and Dahlgren, R.A. (1993) *Volcanic Ash Soils. Genesis, Properties and Utilization*. Developments in Soil Science, **21**. Elsevier, Amsterdam.

Shoval, S. (2004) Deposition of volcanogenic smectite along the southeastern Neo-Tethys margin during the oceanic convergence stage. *Applied Clay Science*, **24**, 299–311.

Singer, A., Zarei, M., Lange, F.M. and Stahr, K. (2004)

Halloysite characteristics and formation in the northern Golan Heights. *Geoderma*, **123**, 279–295.

Soil Conservation Service (1972) Determination of free iron oxides. Pp. 311–312 in: *Methods of Soil Analysis* (C.A. Black, editor). American Society of Agronomy, Madison, Wisconsin.

Soil Survey Staff (2003) *Keys to Soil Taxonomy*, ninth edition. United States Department of Agriculture.

Thornthwaite, C.W. and Mather, J.R. (1957) Instructions and tables for computing potential evapotranspiration and the water balance. *Climatology*, **10**, 181–311.

Ugolini, F.C. and Dahlgren, R.A. (2003) Soil development in volcanic ash. *Global Environmental Research*, **6**, 69–81.

Velde, B. (1992) *Introduction to Clay Minerals. Chemistry, Origins, Uses and Environmental Significance*. Chapman & Hall, London.

Vidales, J.L.M., Sanz, J.L., Guijarro, J., Hoyos, M.A. and Casas, J. (1985) Smectite origins in the volcanic soils of the Calatrava region (central Spain). *5th Meeting of the European Clay Groups, Prague*, pp. 465–470.

Vizcaíno, C., García Gonzàles, M.Z. and García Vicente, J. (1979) Suelos vulcánicos españoles. *Anales Edafologia Agrobiologia*, **XXXVIII**, 431–445.

Wada, K. (1961) Lattice expansion of kaolin minerals by treatment with potassium acetate. *American Mineralogist*, **46**, 78–91.

Wilson, M.J. (1987) Soil smectites and related interstratified minerals: Recent developments. Pp. 167–173 in: *Proceedings of the International Clay Conference 1985* (L.G. Schultz , H. van Olphen and F.A. Mumpton, editors). The Clay Minerals Society, Boulder, Colorado.

WRB (1998) World Reference Base for Soil Resources. World Soil Resources Reports **84**, FAO, Rome.

(*Received 9 March 2004; revised 8 March 2005; Ms. 890; A.E. Helge Stanjek*)